

**ANALYSIS OF O<sub>3</sub> FORMATION DURING A STAGNATION EPISODE IN  
CENTRAL TN IN SUMMER 1995**

**P. H. Daum, L. I. Kleinman, D. Imre, L. J. Nunnermacker, Y.-N. Lee,  
S. R. Springston, and L. Newman  
Environmental Chemistry Division  
Department of Applied Science  
Brookhaven National Laboratory  
Upton, NY 11973**

**J. Weinstein-Lloyd,  
Dept. of Chemistry and Physics,  
SUNY, Old Westbury,  
Old Westbury, NY 11586**

**R. J. Valente, R. E. Imhoff, R. L. Tanner, and J. F. Meagher<sup>1</sup>  
Atmospheric Sciences Department  
Tennessee Valley Authority  
Muscle Shoals, AL 35662**

**Second Revision: July 1999**

**Accepted for publication in  
Journal of Geophysical Research**

<sup>1</sup> Now at Aeronomy Laboratory, National Oceanic and Atmospheric Administration, Boulder, Colorado

By acceptance of this article, the publisher and/or recipient acknowledges the U.S. Government's right to retain a nonexclusive, royalty-free license in and to any copyright covering this paper.

Research by BNL investigators was performed under the auspices of the U.S. Department of Energy under Contract No. DE-AC02-98CH10886.

# Analysis of O<sub>3</sub> formation during a stagnation episode in central Tennessee in summer 1995

P. H. Daum, L. I. Kleinman, D. Imre, L. J. Nunnermacker, Y.-N. Lee, S. R. Springston, and L. Newman

Environmental Chemistry Division, Department of Applied Science, Brookhaven National Laboratory, Upton, New York

J. Weinstein-Lloyd

Department of Chemistry and Physics, State University of New York, Old Westbury

R. J. Valente, R. E. Imhoff, R. L. Tanner, and J. F. Meagher<sup>1</sup>

Atmospheric Sciences Department, Tennessee Valley Authority, Muscle Shoals, Alabama

**Abstract.** O<sub>3</sub> production in the Nashville urban plume during the O<sub>3</sub> episode that occurred on July 11-July 13 1995, is examined to characterize the factors that control the ozone production rate and efficiency, and to examine the relative importance of natural and anthropogenic sources of hydrocarbons to ozone production in the urban center and outlying areas. The analysis focuses on data collected during aircraft flights on July 11 when the Nashville area was sampled more or less continuously from about 1000 to 1800 LT. The instantaneous ozone production rate P(O<sub>3</sub>) in the downtown area from late morning through midafternoon on July 11 ranged between 10 and greater than 30 ppbv/h depending on location. After 1700 local time, production rates dropped to a few ppbv/h owing to the diminished solar intensity. Instantaneous production efficiencies with respect to NO<sub>x</sub> in the downtown area ranged between 2.5 and 8, linearly depending on the ratio of the hydrocarbon to NO<sub>x</sub>, OH reactivity. Integral O<sub>3</sub> production efficiencies corrected for NO<sub>z</sub> losses ranged between 1.5 and 4. The lowest efficiency was observed in the downtown area in the morning where NO<sub>x</sub> concentrations were high and hydrocarbon to NO<sub>x</sub> reactivity ratios were the lowest. Throughout the day, P(O<sub>3</sub>) in the downtown area was limited by the availability of hydrocarbons. Anthropogenic hydrocarbons and CO contributed about 66% of the total hydrocarbon OH reactivity in the downtown area. In the mature urban plume downwind of Nashville, P(O<sub>3</sub>) dropped to 6-9 ppbv/h at midafternoon and was controlled by the availability of NO<sub>x</sub>. Integral O<sub>3</sub> production efficiencies in the mature urban plume ranged between 3.5 and 4. When present in large quantities (1-3 ppbv), isoprene significantly increased both the rate and efficiency of ozone production as long as the photochemical system was not strongly NO<sub>x</sub>-limited.

## 1. Introduction

During the 1995 Southern Oxidants Study (SOS) field study in Nashville, Tennessee [Meagher *et al.*, 1998], a stagnation episode occurred during the period July 11 through July 13, 1995, causing the formation of the highest O<sub>3</sub> concentration observed at the downtown Nashville site during the entire month-long (June 27 to July 20, 1995) intensive. Qualitative aspects of the geographic distribution of O<sub>3</sub> and product species have been described elsewhere [Banta *et al.*, 1998, Valente *et al.*, 1998]. Briefly, the light daytime winds minimized transport of the urban emissions away from the city center during the daylight hours of the episode and allowed the accumulation of O<sub>3</sub> and O<sub>3</sub> precursors in near proximity to the Nashville urban center. On July 12, the day with the lowest wind speeds, the entire Nashville plume at midafternoon encompassed an area only 10 km wide and 20 km in length, only several times larger than the Nashville urban area itself [Valente *et al.*, 1998]. These low wind speeds in combination with high humidity and solar intensity allowed the urban plume to produce very high concentrations of O<sub>3</sub> before the O<sub>3</sub> and O<sub>3</sub> precursors were advected out of the area.

Although daytime wind velocities were light during the episode, it was observed that the inertial oscillation and associated low level jets that occurred during the evening were quite strong [McNider *et al.*, 1998]. These nocturnal jets transported ozone and ozone precursors accumulated in the boundary layer during the previous day out of the immediate Nashville area at night. In effect, this process minimized the accumulation of O<sub>3</sub> over the 3-day period. However,

the nighttime redistribution of O<sub>3</sub> served to increase background concentrations to which next day O<sub>3</sub> production was added [Banta *et al.*, 1998].

Previous papers describing this episode [Banta *et al.*, 1998; Valente *et al.*, 1998] have not examined the ozone formation processes in detail but have been mainly concerned with an analysis of the meteorology, and a qualitative description of the chemistry. Here we examine the details of ozone formation during the episode. The specific goal is to examine the rate and efficiency of O<sub>3</sub> production, NO<sub>x</sub>, and/or VOC limitations to the amount of O<sub>3</sub> produced as a function of time and location, and to compare these quantities to those that were determined for the Nashville urban plume under conditions where the mean wind flow was well defined and the Nashville plume was relatively rapidly advected out of the Nashville area. Details of the latter analysis may be found elsewhere [Nunnermacker *et al.*, 1998; Daum *et al.*, this issue]. This paper focuses on the data collected on July 11, 1995 because of the extensive sampling of the Nashville plume from morning through late afternoon that occurred on this day. Data from July 12 and July 13 are included, as appropriate, to illustrate various aspects of the processing of Nashville emissions during the episode.

---

<sup>1</sup>Now at Aeronomy Laboratory, National Oceanic and Atmospheric Administration, Boulder, Colorado.

## 2. Experiment

### 2.1. Meteorology

A complete description of the meteorology during the episode is given elsewhere [McNider *et al.*, 1998; Banta *et al.*, 1998; Valente *et al.*, 1998]. Briefly, weather during the stagnation period was dominated by a upper level high-pressure system that moved from west to east. The nature of this system with its weak pressure gradients caused the daytime winds to be light and variable; during daylight hours the mean boundary layer flow was less than 2 m/s throughout the episode [Banta *et al.*, 1998]. Although light, the mean flow was from the NE on July 11, the N on July 12, and the SE on July 13. Consequently the Nashville urban plume was transported successively to the SW, South, and NE of the city during the 3-day stagnation period [Valente *et al.*, 1998; McNider *et al.*, 1998]. Although daytime winds were weak and ill defined, at night winds were sufficiently high to transport pollutants accumulated during the day away from the immediate vicinity of Nashville. The high-pressure system also caused strong subsidence which suppressed mixing depths compared to other days in the program when different meteorological conditions prevailed. The midday boundary layer height on July 10 was nearly 3 km, whereas during the episode the boundary layer height never exceeded 2 km [McNider *et al.*, 1998].

### 2.2. Trace Gas and Aerosol Measurements

Details regarding the trace gas and aerosol measurements made aboard the two aircraft can be found elsewhere [Nunnermacker *et al.*, 1998; Valente *et al.*, 1998; Weinstein-Lloyd *et al.*, 1998; Lee *et al.*, 1998; Hübler *et al.*, 1998]. Briefly, nitrogen oxides were measured using a three channel NO/O<sub>3</sub> chemiluminescence instrument; ozone was measured with a commercial UV absorption detector (Thermal Environmental Instruments, Model 49-100); SO<sub>2</sub> was measured with a modified pulsed fluorescence detector (Thermo Environmental Systems, Model 43S); CO was measured with a modified nondispersive infrared detector (Thermal Environmental Systems model 48). Trace gas measurements made atop the Polk building in downtown Nashville are described by Meagher *et al.* [1996].

### 2.3. Aircraft Flights

Flights were made by one or more aircraft on each of the days during the 3-day stagnation period. On July 11 the TVA helicopter made three flights, 1000-1200, 1340-1530, and 1600-1745 local time; a composite flight track is shown in Plate 1a. The helicopter flights focused on characterizing Nashville emissions and the chemical processes that occurred in the source region. The midmorning flight included a vertical profile over the downtown site atop the Polk Building. The ground track of the single G-1 flight on July 11 (1300 and 1552 LT) is shown in Plate 1b. This flight included a vertical profile to the SW of the city, a box pattern around the city outside of the urban area which yielded data on background chemical composition, and a box pattern with diagonals to characterize the chemical composition and spatial distribution of the Nashville plume. A representation of the approximate geographic distribution of the afternoon O<sub>3</sub> plume resulting from processing of Nashville emissions as inferred from the aircraft measurements is superimposed on the flight tracks. Details of the aircraft flights and O<sub>3</sub> distributions for July 12 and July 13 are given by Valente *et al.* [1998].

### 2.4. Model Calculations

The calculations were performed with an observation driven photochemical box model and used steady state approximations as described by Kleinman *et al.* [1997]. The model consists of the kinetic rate expressions for species which are not constrained to their observed values, that is, OH, HO<sub>2</sub>, organic peroxy radicals, and NO<sub>2</sub>. An integration of these equations produces the steady state concentrations of radicals consistent with observed concentrations of stable species. The concentrations of NO, O<sub>3</sub>, CO, SO<sub>2</sub>, H<sub>2</sub>O<sub>2</sub>, and organic peroxide; as well as temperature, dew point, and solar intensity are constrained to their observed (from the aircraft flights) and/or estimated values. The calculations yield the concentrations of fast reacting species including OH, HO<sub>2</sub>, RO<sub>2</sub>, and NO<sub>2</sub> that are in equilibrium with the measured and or estimated mix of stable compounds.

Calculations correspond to the times and locations where hydrocarbon canister samples were collected. Since measurements of HCHO were not made on the helicopter, HCHO concentrations were estimated from measurements made by the G-1 when it flew in approximately the same region. Methyl vinyl ketone (MVK) and methacrolein (MAC), were set at 250 and 110% of isoprene as appropriate for an equilibrium mixture determined by OH reaction kinetics. If equilibrium conditions do not pertain, errors will propagate through our calculations in approximate proportion to the fraction of the hydrocarbon reactivity attributable to MCK and MAC. With the exception of MVK and MAC, contributions of hydrocarbons such as terpenes that were not measured, are not included in our calculations.

## 3. Results and Discussion

### 3.1. Polk Site Measurements

Time plots of O<sub>3</sub>, CO, NO<sub>y</sub>, and wind speed made atop of the Polk building (~110 m above ground level) in downtown Nashville for the period midnight July 11 to midnight July 13, 1995, are presented in Figures 1a-1d. Peak O<sub>3</sub> concentrations, Figure 1a, which occurred early afternoon every day of the episode, were among the highest measured during the entire program; the peak O<sub>3</sub> concentration observed on the afternoon of July 12 was the highest observed on any of the days.

The diurnal pattern of the CO, and NO<sub>y</sub> concentrations during the episode is typical [Kleinman *et al.*, 1998]. CO and NO<sub>y</sub> exhibit daily maxima between 0600 and 0900 in the morning. This early morning peak in concentrations coincides with a burst of emissions from the morning rush hour to a local minimum in the wind speeds, Figure 1d, and to enhanced vertical mixing because of surface heating (local sunrise is at ~0600) which brings fresh emissions to the height of the measurement site. From about 0930-1030 the CO and NO<sub>y</sub> concentrations decrease rapidly. This may be attributed to the rapid growth of the mixed layer diluting emissions trapped close to the surface during the night and early morning with cleaner air from aloft. From midmorning through late evening the CO and NO<sub>y</sub> concentrations decreased slowly. This decrease appears to be controlled by vertical mixing and dilution. Note that the daily minimum in the CO and NO<sub>y</sub> concentrations coincides with the early evening maximum in the wind speed, Figure 1. Overnight concentrations were highly variable depending principally on meteorological factors such as wind speed and vertical mixing.

The O<sub>3</sub> concentrations exhibited a concentration minimum about the same time as the early morning rise in the CO and NO<sub>y</sub> concentrations. This minimum is due to titration of residual O<sub>3</sub> left near the surface overnight by freshly emitted NO. The O<sub>3</sub> concentration starts to rise rapidly at about 0930, coincident with the rapid increase in the height of the mixed layer and consequent decrease in the CO and NO<sub>y</sub> concentrations. *Kleinman et al.* [1998] attributed this rise to the downward mixing of high O<sub>3</sub> from aloft. The afternoon peak in the O<sub>3</sub> concentration appears to be controlled by photochemical formation processes. After sunset (about 2000 LT), the O<sub>3</sub> concentration decreased because of transport due to the higher wind speeds and from titration by NO.

The CO and NO<sub>y</sub> concentrations measured at the Polk site were highly correlated because of the predominance of mobile sources in the downtown area. A plot of CO versus NO<sub>y</sub> for the 3 day episode shown in Figure 2 exhibits a slope, 10.6, that is quite close to the CO/NO<sub>y</sub> emissions ratio of  $9.3 \pm 1.4$  estimated from the entire 40 day data set collected at the Polk site during the program [*Kleinman et al.*, 1998].

### 3.2. July 11 Aircraft Measurements

**3.2.1. Morning.** Vertical profiles of trace gas concentrations measured by the TVA helicopter between 1015 and 1040 directly over the downtown site are shown in Figures 3a through 3f. Concentrations of NO<sub>y</sub>, NO<sub>x</sub>, O<sub>3</sub>, and SO<sub>2</sub> measured at the bottom of the profile were within the range of values measured atop the Polk building (see Figure 1) just below the helicopter. A layer of very high and variable concentrations extended from the bottom of the profile up to about 0.5 km indicating that the nocturnal inversion had eroded to this altitude at the time of the profile (about 1030 local time). The majority of the NO<sub>y</sub> in this layer (~0.8) was present in the form of NO<sub>x</sub>, Figures 3a and 3b, indicating that little photochemical processing producing NO<sub>2</sub> had occurred at the time of this profile. The concentration of NO<sub>2</sub> + O<sub>3</sub>, Figure 3d, was much more uniform than O<sub>3</sub> indicating that much of the variability in the O<sub>3</sub> concentration was due to titration by NO. A high concentration of NO<sub>y</sub>, NO<sub>x</sub>, and SO<sub>2</sub>, Figures 3a, 3b, and 3e, was observed at the very top of this layer consistent with the presence of an elevated power plant plume. The profile also indicated the presence of several additional layers: A layer between 0.5 and 0.7 km containing high concentrations of NO<sub>y</sub> (30 ppbv), Figure 3a, most of which was NO<sub>x</sub> (60%), Figure 3b, but only modest concentrations of O<sub>3</sub> (60 ppbv), Figure 3c. This layer was probably composed of unprocessed emissions left from late afternoon of the previous day. Between 0.7 and 0.95 km a layer containing up to 90 ppbv O<sub>3</sub>, Figure 3c; 10 ppbv of NO<sub>y</sub>, Figure 3a, and almost no NO<sub>x</sub>, Figure 3b, was observed. This layer was obviously remnants of previous day photochemistry owing to the high O<sub>3</sub> and low NO<sub>x</sub> concentration. Above 1 km, pollutant concentrations were much lower and quite uniform. The vertical variation in the volatile organic carbon (VOC) reactivity over the downtown site is shown in Figure 3f. Consistent with a surface source for VOC, the VOC reactivity is highest at the bottom of the profile. At the top of the profile, reactivities are nearly a factor of 10 lower than in the growing boundary layer, no doubt because of a combination of dilution and consumption during O<sub>3</sub> production.

Figure 4 shows the average apportionment of VOC reactivity, here defined as the sum of the OH reactivities of the hydrocarbons measured in the samples collected midmorning in the downtown region by the TVA helicopter. Biogenic hydrocarbons include contributions from isoprene, MVK, and MAC, and 40% of the

HCHO (the fraction estimated from isoprene degradation). The majority of the VOC reactivity may be classified as anthropogenic if both carbon monoxide and anthropogenic hydrocarbons are included. The single largest source of hydrocarbon reactivity is carbon monoxide.

Immediately upon completion of the vertical profile over downtown Nashville, the helicopter sampled the Nashville urban plume about 8 km SSW of the Polk building between 1040 and 1100 LT, Plate 1a. Figure 5a shows crossplume plots of O<sub>3</sub> and CO; Figure 5b shows cross plume plots of NO<sub>x</sub> and NO<sub>y</sub>. As might be expected from the proximity of the measurements to the urban center, precursor concentrations were quite high. The peak concentration of CO was ~780 ppbv and for NO<sub>y</sub> was about 45 ppbv. About 55% of the NO<sub>y</sub> was present as NO<sub>x</sub>. At the edge of the urban plume, O<sub>3</sub> concentrations were about 80 ppbv; in the center they were suppressed by as much as 10-15 ppbv no doubt by titration with fresh NO emissions.

The correlation between CO and NO<sub>y</sub> for measurements obtained during this transect is shown in Figure 5c. The slope of this plot is only marginally higher (11.3 versus 10.6) than the one derived from the Polk site data, both during the episode period and for the entire project, consistent with the minimal amount of photochemical processing that has occurred at the time of these measurements. Such processing would generate NO<sub>x</sub> oxidation products such as HNO<sub>3</sub> which would then be lost by dry deposition and cause the CO/NO<sub>y</sub> ratio to increase. As discussed below, plume measurements made later in the day downwind of Nashville exhibit much higher CO/NO<sub>y</sub> ratios than these because of such losses.

The data from the midmorning helicopter flight over the urban center prior to the formation of substantial amounts of O<sub>3</sub> allow us to examine the initial rates and efficiencies of O<sub>3</sub> formation which we will subsequently compare to the rates, efficiencies, and amount of O<sub>3</sub> in the urban plume after these emissions had been processed for some hours, and generated substantial additional O<sub>3</sub>. The rates and efficiencies are computed for each of the hydrocarbon samples using a box model as described above; locations of the samples are indicated in Plate 1a.

The dependencies of these computed rates and efficiencies are examined in the context of a set of approximate equations derived elsewhere [*Daum et al.*, this issue; *Kleinman et al.*, 1997]. Pertinent relations include equation (1) for the instantaneous ozone production rate,  $P(O_3)$  at low NO<sub>x</sub>; equation (2) for  $P(O_3)$ , and equation (3) for the instantaneous production efficiency with respect to NO<sub>x</sub>, at high NO<sub>x</sub>. Derivation of equation (1), [*Kleinman et al.*, 1995, 1997] starts from the assumption that the ozone production rate can be approximated by the rate at which NO is oxidized to NO<sub>2</sub> by peroxy radicals, that is, that  $P(O_3) = k_t ([HO_2] + [RO_2])[NO]$ . Derivation of equation (2) starts from the assumption that the rate of O<sub>3</sub> production can be approximated by the rate at which OH reacts with hydrocarbons, that is, that  $P(O_3) = k_1 [OH][RH]$  [*Sillman*, 1990, 1995]. Both derivations assume steady state conditions, that PAN concentrations are near equilibrium, and that losses of radicals by processes other than formation of peroxides or HNO<sub>3</sub> are negligible. Equation (1) is most useful for examining the behavior of  $P(O_3)$  at low NO<sub>x</sub> concentrations, while equation (2) is most useful for examining  $P(O_3)$  at high NO<sub>x</sub>. Equation (3) follows directly from equation (2).

$$P(O_3) = \frac{k_t}{(2k_{\text{eff}})^{1/2}} (\varrho)^{1/2} [NO] \quad (1)$$

$$P(\text{O}_3) = Y \frac{k_1[\text{HC}]}{k_2[\text{NO}_2]} Q \quad (2)$$

$$\text{OPE}_x = Y \frac{k_1[\text{HC}]}{k_2[\text{NO}_2]} \quad (3)$$

In (1)-(3),  $k_i$  is the weighted average rate constant for reaction of HO<sub>2</sub> and RO<sub>2</sub> with NO;  $k_{\text{eff}}$  is the effective rate constant for peroxide formation;  $Q$  is the primary radical production rate (i.e., from the photolysis of O<sub>3</sub> and HCHO);  $Y$  is the average yield of [HO<sub>2</sub>]+[RO<sub>2</sub>] for each OH+HC reaction (G. Tonnesen and R. Dennis, private communication, 1999);  $k_2[\text{HC}]$  represents the OH reactivity for the mix of hydrocarbons including CO;  $k_2[\text{NO}_2]$  is the OH reactivity of NO<sub>2</sub>.

Calculated values of the instantaneous ozone production rate,  $P(\text{O}_3)$ , are shown in Figure 6a as a function of the quantity  $Qk_1[\text{HC}]/k_2[\text{NO}_2]$ .  $P(\text{O}_3)$  values range from 10 to approximately 30 ppbv/h driven mostly by variations in  $k_1[\text{HC}]/k_2[\text{NO}_2]$ . The linear dependency on  $Qk_1[\text{HC}]/k_2[\text{NO}_2]$  is characteristic of O<sub>3</sub> formation under high NO<sub>x</sub>, hydrocarbon-limited conditions [Daum *et al.*, this issue]. As pointed out above, the VOC reactivity driving these high production rates originates from anthropogenic sources with biogenics on average contributing about one third of the reactivity. The slope of this plot, which is a function of the hydrocarbon mix, may be interpreted as the average number of peroxy radicals formed by the reaction OH + RH. For these data, the slope implies that an average of 1.5 peroxy radicals are formed each time an OH radical reacts with a hydrocarbon. The calculated fraction of radicals being lost from the photochemical system by forming HNO<sub>3</sub> is 95%. This high fractional loss via HNO<sub>3</sub> formation is characteristic of a system in which  $P(\text{O}_3)$  is hydrocarbon limited [Kleinman *et al.*, 1997].

The instantaneous production efficiency with respect to NO<sub>x</sub>,  $\text{OPE}_x$ , varies linearly with the  $k_1[\text{HC}]/k_2[\text{NO}_2]$ , Figure 6b, again characteristic of O<sub>3</sub> formation under high NO<sub>x</sub>, hydrocarbon limited conditions [Daum *et al.*, this issue].  $\text{OPE}_x$  varies between approximately 2.5 and 6 with the lowest value occurring where the NO<sub>y</sub> concentration is the highest. Net production rates and efficiencies, which take into account O<sub>3</sub> losses, mainly by photolysis, are about 10% lower than the values exhibited in Figure 6. The O<sub>3</sub> production efficiency with respect to the primary radical production rate,  $\text{OPE}_R$ , defined as  $P(\text{O}_3)/Q$ , is nearly identical to  $\text{OPE}_x$  and varies linearly with the quantity  $(k_1[\text{HC}]/k_2[\text{NO}_2])$  (not shown) as expected for high NO<sub>x</sub> conditions [Daum *et al.*, this issue].

**3.2.2. Midafternoon.** By early to midafternoon photochemical processing of the Nashville urban emissions had resulted in an O<sub>3</sub> plume that extended from just east of the city to about 40 km southwest of the city [Valente *et al.*, 1998], see Plate 1. Flights were made by both the helicopter and the G-1 in the downtown area and in the plume downwind of the city. Owing to the continuing admixture of substantial quantities of O<sub>3</sub> precursors, O<sub>3</sub> was being rapidly produced in the downtown area even though substantial excess O<sub>3</sub> had already been formed. O<sub>3</sub> concentrations were somewhat higher in the downwind samples, but production rates were lower because the O<sub>3</sub> precursors had been depleted and fresh emissions were not being mixed into the system. We first describe the downtown measurements.

**3.2.2.1. Downtown measurements:** Trace gas concentrations measured by the G-1 during a transect directly over the downtown area at mid-afternoon are shown in Figures 5d and 5e. At the time of

these measurements, peak O<sub>3</sub> concentrations near the urban center had risen to almost 130 ppbv, about a 60 ppbv increase over the concentration measured over the urban center some 4.5 hours earlier. Although there is some indication in the data of an O<sub>3</sub> contribution from a nearby power plant in a portion of the urban plume (i.e., the presence of an SO<sub>2</sub> plume), generally CO is well correlated with O<sub>3</sub>, indicating that most of the O<sub>3</sub> was produced by urban, rather than power plant NO<sub>x</sub> emissions. As indicated by the NO<sub>y</sub> species plot, Figure 5e, substantial quantities of NO<sub>x</sub>, presumably from fresh emissions, are available for production of additional O<sub>3</sub>. Similar plume characteristics were exhibited by the data from a flight of the TVA helicopter over the city center somewhat earlier in the afternoon.

The CO/NO<sub>y</sub> regression corresponding to the data in Figure 5f exhibits a slope of ~13.2 which is intermediate between the slope characteristic of fresh unprocessed emissions, ~10.6, and the aged urban plume, 19.9 (see next section). The slope is consistent with the addition of fresh CO and NO<sub>y</sub> emissions to an air parcel in which extensive photochemical production of O<sub>3</sub>, accompanied by attendant formation and loss of NO<sub>z</sub>, has already occurred.

$P(\text{O}_3)$  over downtown Nashville in the midafternoon ranged between 15 and 22 ppbv/h and varied linearly with  $k_1[\text{HC}]/k_2[\text{NO}_2]$  consistent with HC-limited chemistry, Figure 6a.  $\text{OPE}_x$  ranged between 4 and 8, Figure 6b, with the highest value exhibited in a region where 1 ppbv of isoprene was measured. The fraction of radicals being terminated as HNO<sub>3</sub> was ~90% indicating that similar to the morning,  $P(\text{O}_3)$  was hydrocarbon-limited.

**3.2.2.2. Downwind measurements:** The G-1 sampled the mature urban plume downwind of Nashville numerous times during the afternoon, Plate 1b. The chemical properties of the urban plume were very uniform from place to place. These properties are illustrated in Figures 5g and 5h which show trace gas data from a G-1 transect of the urban plume about 40 km SW of Nashville. The peak O<sub>3</sub> concentration, Figure 5g, was about 130 ppbv and was associated with a peak CO concentration of ~300 ppbv. The NO<sub>y</sub> plot exhibited two sharp peaks associated with peaks in the NO<sub>x</sub> concentration and a broader peak of about 10 ppbv correlated with the peak in the O<sub>3</sub> concentration. Review of the flight track indicates that the NO<sub>x</sub> peaks were associated with passage of the aircraft over a major interstate highway (I-65). The peak NO<sub>x</sub> concentration, corresponding to the peak O<sub>3</sub> concentration, is 1 ppbv and represents about 10% of the concurrently measured NO<sub>y</sub>. The relatively low NO<sub>x</sub> concentration may be taken as an indication that O<sub>3</sub> production is nearly complete. NO<sub>y</sub> and CO were highly correlated during this and several other transects of the urban plume SW of the city. The regression plot for this transect, Figure 5i, exhibited a slope of 19.9 and an  $r^2$  of 0.94.

Similar concentrations and correlations were exhibited by the data from a transect of the helicopter through the urban plume made at about the same time but 10 km closer to Nashville. The peak O<sub>3</sub> concentration was ~130 ppbv, essentially identical to that measured on the G-1, and was associated with an NO<sub>y</sub> concentration of ~13 ppbv and a NO<sub>x</sub> concentration of ~1-2 ppbv. CO measurements were not available.

Values of  $P(\text{O}_3)$  averaged 9 ppbv/h in the plume were comparable to background values of  $P(\text{O}_3)$  which ranged between 6 and 9.5 ppbv/h. Since the primary radical production rate  $Q$  was comparable to late morning conditions in the downtown area, the lower values of  $P(\text{O}_3)$  in comparison to the late morning downtown values may be attributed to the much lower NO<sub>x</sub> and hydrocarbon concentrations.

NO<sub>x</sub> in the aged urban plume averaged 1.1 ppbv, compared to ~16 ppbv in the fresh urban plume at midmorning; hydrocarbon reactivity decreased by about 40% on average. These changes in concentration can be attributed to a combination of dilution, because of the growth of the boundary layer from morning through afternoon, and to consumption of these precursors during formation of O<sub>3</sub>.

Although  $P(O_3)$  is significant in the downwind plume, and there are still sufficient precursors to form additional O<sub>3</sub>, the character of the O<sub>3</sub> formation process has changed. This is illustrated by Figure 7 which shows  $P(O_3)$  as a function of the  $[NO]Q^{1/2}$  for the aged urban plume samples as well as several background samples. The observed linear dependency is a feature of O<sub>3</sub> production under NO<sub>x</sub>-limited conditions. This contrasts to the O<sub>3</sub> production in the downtown area which was HC-limited in the morning and remained HC-limited in the afternoon. Another strong indicator of NO<sub>x</sub> sensitivity is the high fraction of radicals terminating in the formation of peroxides (averaging 88%), leading to peroxide formation rates that average 0.7 ppbv/h.  $OPE_x$  for these samples was high ranging between 12 and 18 ppbv/ppbv, characteristic of a low NO<sub>x</sub> environment where losses of NO<sub>x</sub> by formation of HNO<sub>3</sub> are minimized because of the low NO<sub>2</sub> and OH concentrations.  $OPE_R$  for these samples is quite low because a high fraction of the radicals form peroxides rather than reacting with NO to form O<sub>3</sub>.

**3.2.3. Late afternoon.** Properties of the downtown urban plume observed during a late afternoon (1600-1730 local time) helicopter flight were very similar to the those observed at midafternoon except for the ozone production rate. The maximum downtown O<sub>3</sub> concentration was about 105 ppbv and was associated with NO<sub>y</sub> concentrations of 20 ppbv, NO<sub>x</sub> of 8 ppbv, and a CO concentration of about 600 ppbv.  $P(O_3)$  was low at 2.4 ppbv/h because the reduced late afternoon solar intensity decreased  $Q$  to values less than 1 ppbv/h. Ozone production was hydrocarbon-limited with greater than 95% of the radicals terminating in the formation of HNO<sub>3</sub>.  $P(O_3)$  fell within the ensemble of downtown samples when plotted as a function of  $Qk_1[HC]/k_2[NO_2]$ , Figure 6a, indicating that O<sub>3</sub> production had similar character in the downtown area throughout the day. The apportionment of hydrocarbon reactivity between anthropogenic and biogenic sources was very nearly the same as observed in the downtown area during the morning flight.

### 3.3. Aircraft Measurements on July 12 and 13

On July 12, the TVA helicopter made three flights, mid-morning, early, and late afternoon. The midmorning vertical profile of trace gases over the downtown site at ~1000 LT (not shown) was quite similar to the early morning trace gas profile for July 11 with very high concentrations of NO<sub>y</sub>, a high fraction of which is NO<sub>x</sub> at altitudes of 500 m and below, a well defined layer of NO<sub>y</sub> at ~650-900 m, and a very thin layer just above 1000 m. The corresponding O<sub>3</sub> profile was somewhat more uniform than the NO<sub>y</sub> profile with 50-60 ppbv in the lowest two layers and up to 80 ppbv above 1000 m.

Owing to the very light winds from the north, Nashville emissions did not move significantly outside the metropolitan area during the daylight hours of July 12. Because of this, maximum O<sub>3</sub> concentrations were very high and were located very near the center of the urban area; the bulk of the urban plume only extended about 15 km south of the city [Valente *et al.*, 1998]. Plots of O<sub>3</sub> and related trace gases measured in midboundary layer, about 5 km downwind of downtown Nashville, during midafternoon are shown in Figure 8. The peak O<sub>3</sub> concentration measured during this transect, of 160 ppbv, was the highest measured during the entire project. Note in the

panel depicting NO<sub>y</sub> and NO<sub>x</sub> that substantial NO<sub>x</sub> remains to produce additional O<sub>3</sub>. Detailed calculations of the  $P(O_3)$  and related quantities were not performed because of the lack of CO data and because of the small number of hydrocarbon samples that were collected during this flight.

There were no morning flights on July 13. The urban plume was sampled by the G-1 about 25 km to the NNW of Nashville at various times between 1330 and 1430 local time at altitudes of 1150, 700, and 450 m mean sea level (msl). Properties of the urban plume at all three altitudes were very similar, exhibiting peak O<sub>3</sub>, CO, and NO<sub>y</sub> concentrations that were nearly identical to each other. The plume transect at 1150 m, which was near the top of the boundary layer, clearly indicated that this altitude was close to the maximum altitude to which the urban plume had mixed. Concentrations were very high in the Nashville plume at this time and location. Peak O<sub>3</sub> concentrations were about 145 ppbv and were associated with peak CO and NO<sub>y</sub> concentrations of 475 and 17 ppbv, respectively. NO<sub>x</sub> concentrations were approximately 2 ppbv indicating that O<sub>3</sub> production was nearly complete. The regression slope for CO versus NO<sub>y</sub> was 17 ( $r^2=0.93$ ). Similar chemical properties were exhibited by the urban plume sampled by the TVA helicopter 5-8 km downwind of Nashville (not shown) at about the same time as the G-1 flight. The peak O<sub>3</sub> concentration was about 145 ppbv, and peak NO<sub>y</sub> was about 15 ppbv; NO<sub>x</sub> was about 3.5 ppbv, and CO was about 425 ppbv. The CO/NO<sub>y</sub> regression yielded a slope of 17 ( $r^2 = 0.93$ ). As with the flight of July 12, calculations of  $P(O_3)$  and related quantities were not made because of the small number of hydrocarbon samples that were collected over a very constrained set of conditions.

### 3.4. CO-NO<sub>y</sub> Relationships and Their Variation With Plume Age

In this section we examine variations in the relationship between CO and NO<sub>y</sub> in the Nashville plume as it ages. As shown in Figures 5c, 5f, and 5i, the slopes of plots of NO<sub>y</sub> versus CO systematically decrease as the Nashville plume ages and advects downwind. A summary of the data for the plume transects of July 11 as well as selected transects through the urban plume on July 13 are given in Table 1. The data are ordered by the NO<sub>x</sub>/NO<sub>y</sub> ratio which is an indicator of the extent of photochemical processing that has occurred in the plume. Examination of Table 1 shows that CO/NO<sub>y</sub> regression slope systematically increases as the ratio NO<sub>x</sub>/NO<sub>y</sub> decreases. Since CO may be considered to be conserved over the timescales of concern here, the increase in the CO/NO<sub>y</sub> ratio may be attributed to losses of NO<sub>x</sub> oxidation products from the atmosphere by dry deposition or by conversion of NO<sub>x</sub> to substances that are not measured by the NO<sub>y</sub> instrument. In the work of Nunnermacker *et al.* [1998], we attributed these losses to dry deposition and inferred from the loss rates a dry deposition velocity for HNO<sub>3</sub> from the boundary layer of the order of 5 cm/s. In the next section we will use these CO/NO<sub>y</sub> ratios to correct for NO<sub>z</sub> losses in estimating integral values of  $OPE_x$ .

### 3.5. Integral Ozone Production Efficiencies

The time average, or integral O<sub>3</sub> production efficiency with respect to NO<sub>x</sub> emissions, can be estimated from the slope of a plot of O<sub>3</sub> versus NO<sub>z</sub> corrected for the amount of NO<sub>z</sub> that has been lost in transit from the source region to the point at which the plume is sampled [Nunnermacker *et al.*, 1998]. The magnitude of this loss term can be approximated from the difference between the slopes of

regressions between CO and NO<sub>y</sub> in the source region and at the downwind location where the urban plume was sampled.

Table 1 shows estimates of the integral ozone production efficiency, IOPE<sub>x</sub>, corrected for losses of NO<sub>z</sub>. Efficiencies range from 1.5 for data collected late morning on July 11 in the source region to between 3.5 and 4 in the mature urban plumes sampled on July 11 and July 13. Data from the July 12 flights are not included because of the lack of CO data with which to correct for NO<sub>z</sub> losses. The uncorrected efficiencies (the raw O<sub>3</sub>/NO<sub>z</sub> slopes) increase with decreasing NO<sub>x</sub> concentration. To the extent that the NO<sub>x</sub> concentrations represent a measure of plume age, this trend is consistent with higher fractional losses of NO<sub>z</sub> (mainly HNO<sub>3</sub>) as the plume ages and advects downwind, and reinforces the need to correct for NO<sub>z</sub> losses in estimating IOPE<sub>x</sub>.

The general trend of increasing IOPE<sub>x</sub> with plume age is similar to observations on other days and is a reflection of the more efficient use of NO<sub>x</sub> in O<sub>3</sub> production as the NO<sub>x</sub> concentration decreases. At high NO<sub>x</sub>, NO<sub>2</sub> effectively competes with HC for the OH radical forming HNO<sub>3</sub> thus removing NO<sub>x</sub> from the ozone production cycle. At low NO<sub>x</sub>, nitrate formation is minimized because both OH and NO<sub>2</sub> are low, and while  $P(O_3)$  is small, NO<sub>x</sub> is used very efficiently.

The estimates of IOPE<sub>x</sub> during the episode period are the same, to within the estimated uncertainty, as those derived for the Nashville urban plume from the data collected on July 3 and July 18 [Nunnermacker *et al.*, 1998] when peak O<sub>3</sub> concentrations were lower, and winds were much higher, the latter causing relatively rapid advection of the urban plume away from the city center. The similarity of the O<sub>3</sub> production efficiencies under these very different meteorological conditions supports the view that the details of the chemistry of O<sub>3</sub> production do not vary dramatically with the plume dispersion rate and that the differences in maximum O<sub>3</sub> concentration are due principally to differences in dilution.

### 3.6. Effect of Isoprene on $P(O_3)$ and Related Quantities

Since isoprene has been identified as a major source of VOC reactivity in the SE United States, and in particular has been shown to be an important contributor to regional O<sub>3</sub> production during the 1995 Nashville intensive [Roberts *et al.*, 1998], we examine here the effect of isoprene on O<sub>3</sub> production in the Nashville urban plume. The effect is explored by comparing  $P(O_3)$  and related quantities calculated using measured concentrations of isoprene to calculations in which the isoprene concentration is set to zero. In the "zero isoprene case," we assume that the concentration of methyvinylketone and methacrolein are zero as well, but that the concentration of HCHO decreases by only 40%. The latter assumption is made because isoprene is not the only source of formaldehyde, and we estimate, based upon an apportionment of formaldehyde sources in the SOS study [Lee *et al.*, 1998], that the fraction due to biogenic sources is about 40%.

The first set of calculations corresponds to all of the hydrocarbon samples that were collected in the downtown area on July 11. The effect of setting the isoprene to zero on O<sub>3</sub> production is illustrated in the left-hand panel of Figure 9. Not surprisingly, because O<sub>3</sub> production is HC-limited,  $P(O_3)$  decreases in the "zero isoprene case." The decrease in  $P(O_3)$ , is in approximate proportion to the contribution of isoprene to the total hydrocarbon reactivity in the unperturbed sample. For this set of samples the average isoprene contribution to the total hydrocarbon reactivity and the reduction in  $P(O_3)$  when it is removed is about 30%. Associated with the decrease in  $P(O_3)$  is a decrease in OPE<sub>x</sub> of about 25% which is as

expected since in the HC-limited regime, OPE<sub>x</sub> is proportional to the ratio of the HC to NO<sub>x</sub>, OH reactivity. The fraction of radicals terminated as HNO<sub>3</sub> (%R + NO<sub>x</sub>) is not significantly affected by the change in the isoprene concentration as  $P(O_3)$  is even more HC-limited when isoprene is removed.

The right-hand panel of Figure 9 shows the effect of decreasing the isoprene concentration for a measurement collected at the boundary of the urban plume where the isoprene concentration was very high (3.4 ppbv), representing about 80% of the total hydrocarbon reactivity. As shown in the right-hand panel of Figure 9, setting the isoprene concentration to zero for this sample has a dramatic effect.  $P(O_3)$  decreases by approximately a factor of 2, OPE<sub>x</sub> drops by nearly a factor of 3, and  $P(O_3)$  shifts from being nominally NO<sub>x</sub> sensitive to being nominally HC sensitive. Because ozone production is occurring in a region where the system is in transition between NO<sub>x</sub> and HC-limited chemistry, the effect of reducing isoprene on  $P(O_3)$  is decidedly nonlinear. For the mature urban plume and the background where O<sub>3</sub> production is limited by the availability of NO<sub>x</sub>, variation in the isoprene concentration has only a small effect on the rate and efficiency of ozone production.

Two aspects of the influence of isoprene on O<sub>3</sub> formation rates and efficiencies deserve further discussion. First, we note that isoprene sources are not evenly distributed geographically in central Tennessee [Williams *et al.*, 1997] and thus the contribution of isoprene to the total hydrocarbon mix producing O<sub>3</sub> will vary from location to location. Since the downtown area is not heavily vegetated, we do not anticipate, nor do our data suggest, that this area is a major isoprene source region. However, outside of the downtown area, isoprene emissions may be high depending on the type and density of the tree cover in a given locale. For these reasons, incorporation of isoprene emissions on a scale important to urban O<sub>3</sub> formation is a formidable challenge for modelers. Second, on the basis of the analysis presented at the beginning of this section, the importance of isoprene as a hydrocarbon source for ozone production depends greatly on the state of the photochemical system into which it is emitted. If it is emitted into a system in which  $P(O_3)$  is NO<sub>x</sub>-limited as is the case in the mature Nashville urban plume and for most of the background surrounding Nashville (power plant plumes excepted), then isoprene emissions will have little effect on the rate and quantity of O<sub>3</sub> that is produced since  $P(O_3)$  under these conditions is insensitive to changes in hydrocarbon concentrations. If, however, isoprene is emitted into the photochemical system when NO<sub>x</sub> concentrations are high and  $P(O_3)$  is HC-limited, the effect on both the rate and quantity of O<sub>3</sub> produced can be dramatic.

### 3.7. Dependence of $P(O_3)$ on Changes in NO<sub>x</sub> and Hydrocarbon Concentrations

The sensitivity of the maximum O<sub>3</sub> concentration to changes in NO<sub>x</sub> and HC emissions during the July 11-13 episode has been the subject of a modeling study and is discussed elsewhere [Sillman *et al.*, 1998]. Briefly, it was concluded that production of the maximum O<sub>3</sub> concentration in the Nashville urban plume during this episode occurred under conditions that may be best described as at the transition between NO<sub>x</sub> and hydrocarbon-limited conditions. Furthermore, it was found that the maximum O<sub>3</sub> concentration was quite insensitive to changes in either NO<sub>x</sub> or hydrocarbon emissions. A 35% decrease in regional NO<sub>x</sub> emissions only lowered the maximum above background O<sub>3</sub> concentration (40 ppbv) by 19%. A similar decrease in the O<sub>3</sub> concentration was found for a 35% change in VOC emissions.

Here we address the effect of changes in NO<sub>x</sub> and VOC concentrations on  $P(O_3)$ , focusing on the July 11 data. The procedure that is used is detailed by Kleinman *et al.* [1997]. Briefly, the effects of changing NO<sub>x</sub> or hydrocarbon concentrations are determined by examining the difference between a calculation of  $P(O_3)$  driven by ambient concentrations, and calculations in which the concentration of NO<sub>x</sub> or hydrocarbons is incremented by 10%.

The results of these calculations are shown in Figure 10. The ordinate of Figure 10 is the relative sensitivity of  $P(O_3)$  to changes in NO<sub>x</sub> or hydrocarbon concentrations. The meaning of the relative sensitivity parameter is as follows: If the value of the relative sensitivity is 1, this means that an n% change in either NO<sub>x</sub> or hydrocarbons will result in an n% change in  $P(O_3)$ . If the sensitivity parameter is <1, then there will be smaller than a proportionate change in  $P(O_3)$ ; a negative value of the sensitivity parameter means that decreasing NO<sub>x</sub> or HC will result in an increase in  $P(O_3)$ . The sensitivity parameter is plotted as a function the quantity (%R + NO<sub>x</sub>) which is the percentage of radicals being removed by reaction with NO or NO<sub>2</sub>, which will depend on the NO<sub>x</sub> concentration, and the HC/NO<sub>2</sub> reactivity ratio. The vertical line at a %R + NO<sub>x</sub> of 50% denotes the transition between hydrocarbon and NO<sub>x</sub> sensitive O<sub>3</sub> production.

Several features of this plot stand out. First, all of the samples in the downtown region fall within the hydrocarbon sensitive region of the plot regardless of whether they were collected in the midmorning, mid, or late afternoon. In other words, O<sub>3</sub> formation chemistry on July 11 in the downtown region appears to start out HC sensitive in the morning and to remain that way for the rest of the day. Second, the majority of the samples are in a regime (i.e., those for which %R+NO<sub>x</sub> > 70) where a decrease in the NO<sub>x</sub> concentration will cause an increase in  $P(O_3)$ . Third, we note that except for those samples where %R+NO<sub>x</sub> approaches 1,  $P(O_3)$  is not very sensitive to changes in either NO<sub>x</sub> or hydrocarbon emissions.

Implications of this analysis of the instantaneous chemistry on potential O<sub>3</sub> control strategies for the Nashville nonattainment region are not straightforward. If the issue is O<sub>3</sub> control in the downtown area for stagnation conditions when O<sub>3</sub> is a maximum, then a strategy based on controlling hydrocarbon emissions might be appropriate. From our measurements, anthropogenic hydrocarbons constitute nearly 60% of the hydrocarbon reactivity in the downtown area and would seem to be amenable to control. A strategy based upon NO<sub>x</sub> control would not be effective because  $P(O_3)$  is hydrocarbon-limited, and because of the generally negative sensitivity of  $P(O_3)$  to a decrease in the NO<sub>x</sub> concentration. If the issue is O<sub>3</sub> control over the entire nonattainment area, a different strategy might be warranted because of the increased importance of natural sources of hydrocarbons for O<sub>3</sub> production. Obviously, the determination of an effective control strategy is well beyond the scope of this analysis and will require use of a much more sophisticated simulation to develop. However, our analysis does point out that to develop an effective control strategy, simulations must be driven by high-resolution emissions inventories that accurately reflect the spatial distribution of sources of anthropogenic NO<sub>x</sub> and hydrocarbons, as well biogenic hydrocarbons.

#### 4. Summary and Conclusions

O<sub>3</sub> production in the Nashville urban plume during the O<sub>3</sub> episode that occurred on July 11-July 13, 1995, has been examined to characterize  $P(O_3)$ , factors that control the efficiency of O<sub>3</sub>

production, the relative importance of natural and anthropogenic sources of ROG, and to compare these results to a similar analysis that was done on nonstagnation days when the Nashville urban plume was advected rapidly away from the urban center [Nunnermacker *et al.*, 1998].

During the July 11-July 13 episode the Nashville urban plume was sampled over a wide range of conditions. The most complete coverage was obtained on July 11 with aircraft flights over the urban center and downwind occurring from about 1000 to about 1800 LT. Less complete coverage was obtained on July 12 when only the helicopter flew and on July 13 when the urban plume was sampled for only a short period of time in the early afternoon. The chemical properties of the Nashville urban plume during various days of the episode were very similar to each other and to the properties of the plume observed on nonepisodic days except for differences in peak concentrations.

CO/NO<sub>y</sub> emissions ratios as estimated from CO/NO<sub>y</sub> data collected by aircraft over the city center and slightly downwind on the morning of July 11 were quite close to estimates derived from downtown site data for the entire project period [Kleinman *et al.*, 1998] suggesting that the emissions during the episode were similar to those on nonstagnation days. The CO/NO<sub>y</sub> slope increased with increasing plume age consistent with the NO<sub>z</sub> loss rates found on other days.

The instantaneous ozone production rate  $P(O_3)$  over the urban center mid to late morning on July 11 varied linearly with the hydrocarbon/NO<sub>x</sub>, OH reactivity and ranged between 10 and greater than 30 ppbv/h.  $P(O_3)$  in the downtown area was limited by the availability of hydrocarbons throughout the day.  $P(O_3)$  dropped to 6-10 ppbv in the mature urban plume downwind of the city at midafternoon consistent with lower NO<sub>x</sub> and hydrocarbon concentrations due to their consumption in ozone production. Downwind,  $P(O_3)$  varied linearly with the quantity  $[NO]Q^{1/2}$ , characteristic of NO<sub>x</sub>-limited ozone production.  $P(O_3)$  was very sensitive to isoprene. The highest value of  $P(O_3)$ , 35 ppbv/h, corresponded to trace gas concentrations measured at the edge of the urban plume where NO<sub>x</sub> concentrations were modest (4 ppbv), but where the measured isoprene concentration was 3.4 ppbv.

In the downtown area where NO<sub>x</sub> concentrations were high, the instantaneous OPE<sub>x</sub> varied linearly with the NO<sub>x</sub>/HC reactivity ratio and ranged between 2.5 and 6. In the photochemically aged plume where O<sub>3</sub> concentrations were high and NO<sub>x</sub> concentrations low, the instantaneous efficiency was quite high ranging from 12 to 16. The high OPE<sub>x</sub> at low NO<sub>x</sub> was attributed to the very high VOC/NO<sub>x</sub> ratios and the low NO<sub>x</sub> concentration, the latter minimizing losses of NO<sub>2</sub> by formation of HNO<sub>3</sub>. Under high NO<sub>x</sub> conditions the O<sub>3</sub> production efficiency with respect to primary radical production, OPE<sub>R</sub>, was low and nearly identical to OPE<sub>x</sub>; OPE<sub>R</sub> decreased to very low values in the mature urban plume. This was attributed to the diversion of radicals from O<sub>3</sub> to peroxide formation at low NO<sub>x</sub>.

Integral O<sub>3</sub> production efficiencies corrected for NO<sub>z</sub> losses derived from cross-plume data ranged between 1.5 and 4. The lowest efficiency was observed in the downtown area in the morning where NO<sub>x</sub> concentrations were high and HC/NO<sub>x</sub> reactivity ratios were lowest. In the photochemically mature Nashville plume, where maximum O<sub>3</sub> concentrations were observed, the integral efficiencies were between ~3.5 and 4, nearly identical to the efficiencies observed in the mature urban plumes sampled on July 3 and July 18. The latter is supportive of the notion that there are no large differences in the chemistry of O<sub>3</sub> production between episode and nonepisode days.

The hydrocarbon reactivity in the urban center was dominated by anthropogenic hydrocarbons and CO, representing about two thirds of the total hydrocarbon OH reactivity. Downwind of the city, spikes of HC reactivity were observed and were attributed to the addition of fresh isoprene emissions to the urban plume. The observation of hydrocarbon-limited O<sub>3</sub> production in the downtown area throughout the day, coupled with the dominance of anthropogenic sources of hydrocarbons, suggests a hydrocarbon-based strategy for controlling O<sub>3</sub> concentrations in the downtown area during episodic conditions when winds are stagnant. Outside of the downtown area, no obvious strategy for controlling O<sub>3</sub> concentrations under these conditions emerges from our analysis.

**Acknowledgments.** This study was supported by funding from the Department of Energy through the DOE Atmospheric Chemistry Program and from the Environmental Protection Agency through the SOS program. This research was performed under sponsorship of the US Department of Energy under contracts DE-AC02-98CH10886 and DE-AC06-76RLO 1830.

## References

- Banta, R. M., et al., Daytime buildup and nighttime transport of urban ozone in the boundary layer during a stagnation episode, *J. Geophys. Res.*, *103*, 22,519-22,544, 1998.
- Daum, P. H., L. I. Kleinman, D. Imre, L. Nunnermacker, S. Springston, Y.-N. Lee, J. Lloyd, and L. Newman, Analysis of the processing of Nashville urban emissions on July 3 and July 18, 1995, *J. Geophys. Res.*, this issue.
- Hübner, G., et al., An overview of the airborne activities during the SOS 1995 Nashville/Middle Tennessee Ozone Study, *J. Geophys. Res.*, *103*, 22,245-22,260, 1998.
- Kleinman, L., Y.-N. Lee, S. R. Springston, J. H. Lee, L. Nunnermacker, J. Weinstein-Lloyd, X. Zhou, and L. Newman, Peroxy radical concentration and ozone formation rate at a rural site in the southeastern United States, *J. Geophys. Res.*, *100*, 7263-7273, 1995.
- Kleinman, L. I., P. H. Daum, J. H. Lee, Y.-N. Lee, L. J. Nunnermacker, S. R. Springston, L. Newman, J. Weinstein-Lloyd, and S. Sillman, Dependence of ozone production on NO and hydrocarbons in the troposphere, *Geophys. Res. Lett.*, *24*, 2299-2302, 1997b.
- Kleinman, L. I., P. H. Daum, D. G. Imre, C. Cardelino, K. J. Olszyna, and R. G. Zika, Trace gas concentrations and emissions in downtown Nashville during the 1995 SOS/Nashville Intensive, *J. Geophys. Res.*, *103*, 22,545-22,554, 1998b.
- Lee, Y.-N., et al., Atmospheric chemistry and distribution of formaldehyde and several multioxygenated carbonyl compounds during the 1995 Nashville/Middle Tennessee Ozone Study, *J. Geophys. Res.*, *103*, 22,449-22,462, 1998.
- McNider, R. T., W. B. Norris, A. J. Song, R. L. Clymer, S. Gupta, R. M. Banta, R. J. Zamora, and M. Trainer, Meteorological conditions during the 1995 SOS Nashville/Middle Tennessee Field Intensive, *J. Geophys. Res.*, *103*, 22,225-22,260, 1998.
- Meagher, J. F., W. J. Parkhurst, and J. L. Christ, The SOS Nashville/Middle Tennessee Ozone Field Study data base, Tenn. Val. Auth., Environ. Res. Cent., July 16, 1996.
- Meagher, J. F., E. B. Cowling, F. C. Fehsenfeld, and W. J. Parkhurst, Ozone formation and transport in the southeastern United States: An overview of the SOS Nashville/Middle Tennessee Ozone Study, *J. Geophys. Res.*, *103*, 22,213-22,224, 1998.
- Nunnermacker, L. J., et al., Characterization of the Nashville urban plume on July 3 and July 18, 1995: O<sub>3</sub> production efficiency, kinetic analysis, and hydrocarbon apportionment, *J. Geophys. Res.* (in press).
- Roberts, J. M., et al., Measurements of PAN, PPN, and MPAN made during the 1994 and 1995 Nashville intensives of the Southern Oxidants Study, *J. Geophys. Res.*, *103*, 22,473-22,490, 1998.
- Sillman, S., J. A. Logan, and S. C. Wofsy, The sensitivity of ozone to nitrogen oxides and hydrocarbons in regional ozone episodes, *J. Geophys. Res.*, *95*, 1837-1851, 1990.
- Sillman, S., The use of NO<sub>x</sub>, HCHO, H<sub>2</sub>O<sub>2</sub>, and HNO<sub>3</sub> as indicators for ozone-NO<sub>x</sub>-hydrocarbon sensitivity in urban locations, *J. Geophys. Res.*, *100*, 14,175-14,188, 1995.
- Sillman, S., D. He, M. Pippin, P. H. Daum, J. H. Lee, L. Kleinman, and J. Weinstein-Lloyd, Model correlations for ozone, reactive nitrogen and peroxides for Nashville in comparison with measurements: Implications for O<sub>3</sub>-NO<sub>x</sub>-hydrocarbon chemistry, *J. Geophys. Res.*, *103*, 22,629-22,644, 1998.
- Valente, R. J., R. E. Imhoff, R. L. Tanner, J. F. Meagher, P. H. Daum, R. M. Hardesty, R. M. Banta, R. J. Alvarez, R. McNider, and N. Gillani, Ozone production during an urban air stagnation episode over Nashville, Tennessee, *J. Geophys. Res.*, *103*, 22,555-22,568, 1998.
- Weinstein-Lloyd, J., J. H. Lee, P. H. Daum, L. I. Kleinman, L. J. Nunnermacker, S. R. Springston, and L. Newman, Measurements of peroxides and related species during the 1995 summer intensive of the Southern Oxidants Study in Nashville, Tennessee, *J. Geophys. Res.*, *103*, 22,361-22,374, 1998.
- Williams, J., et al., Regional ozone from biogenic hydrocarbons, deduced from airborne measurements of PAN, PPN, and MPAN, *Geophys. Res. Lett.*, *24*, 1099-1102, 1997.
- P. H. Daum, D. Imre, L. I. Kleinman, Y.-N. Lee, L. Newman, L. J. Nunnermacker, and S. R. Springston, Environmental Chemistry Division, Department of Applied Science, Brookhaven National Laboratory, Upton, NY 11973. (phdaum@bnl.gov)
- R. E. Imhoff, J. F. Meagher<sup>1</sup>, R. L. Tanner, and R. J. Valente, Atmospheric Sciences Department, Tennessee Valley Authority, Muscle Shoals, AL 35662.
- J. Weinstein-Lloyd, Department of Chemistry and Physics, SUNY, Old Westbury, NY 11586.

**Table 1.** Estimates of OPE<sub>x</sub> during the July 11-13 O<sub>3</sub> Episode in Nashville

Date/ Time (Local)	Platform	Distance from Nashville, km	CO/NO <sub>y</sub> Slope (r <sup>2</sup> )	NO <sub>x/y</sub> (Peak)	O <sub>3</sub> (Maximum), ppbv	NO <sub>x</sub> * (Maximum), ppbv	O <sub>3</sub> /NO <sub>z</sub> Slope (r <sup>2</sup> )	IOPE <sub>x</sub>
July 11- July 13	Polk Site	0	11.6 (0.94)	NA	----	----	----	----
July 11 (1030)	TVA	0	11.3 (0.78)	0.55	92	23	1.5 (0.32)	1.5
July 11 (1500)	G-1	0	13.2 (0.93)	0.39	130	9	4.4 (0.80)	3.5
July 13 (1430)	TVA	5-8	16.5 (0.76)	0.24	145	3.5	6.5 (0.94)	4
July 13 (1430)	G-1	25	17 (0.93)	0.12	145	2	5.9 (0.98)	3.5
July 11 (1500)	G-1	30	23 (0.92)	0.09	130	1.2	8.4 (0.95)	4

\*NO<sub>x</sub> concentration corresponding to the maximum O<sub>3</sub> concentration.

## Figure Captions

**Plate 1.** Ground tracks of aircraft flights on July 11, 1995. Shaded area represents the approximate dimensions of the Nashville O<sub>3</sub> plume. Contour is drawn at an O<sub>3</sub> concentration of 100 ppbv. (a) TVA helicopter flights; (b) G-1 Flights. Green symbols indicate location of the hydrocarbon samples.

**Figure 1.** Concentrations of trace species (5 min averages) measured at the Polk Building site in downtown Nashville during the July 11-13 ozone episode. (a) O<sub>3</sub>; (b) CO; (c) NO<sub>y</sub>; (d) Wind speed

**Figure 2.** Regression plot of NO<sub>y</sub> versus CO for the Polk Building data in downtown Nashville during the 3-day July 11-13, 1995 O<sub>3</sub> episode.

**Figure 3.** Vertical profiles of trace species measured by the TVA helicopter over the Polk Building site in downtown Nashville between 1015 and 1035 LT July 11, 1995. (a) NO<sub>y</sub>; (b) NO<sub>x</sub>; (c) O<sub>3</sub>; (d) O<sub>3</sub> + NO<sub>2</sub>; (e) SO<sub>2</sub>; (f) hydrocarbon reactivity.

**Figure 4.** Apportionment of hydrocarbon OH reactivity for samples collected by the TVA helicopter over downtown Nashville midmorning in the boundary layer on July 11, 1995. Biogenic reactivity includes contributions from isoprene, methylvinylketone, methacrolein, and 40% of the formaldehyde.

**Figure 5.** Properties of the Nashville urban plume measured on July 11, 1995 by the DOE G-1 aircraft and the TVA helicopter. Figures 5a and 5b show cross-plume trace gas concentrations about 5 km downwind of the center of Nashville between 1040 and 1055 LT. Note the absence of a well defined O<sub>3</sub> peak corresponding to the peaks in the CO and NO<sub>y</sub> concentrations, Figure 5c shows the correlation plot between NO<sub>y</sub> and CO. Figures 5d and 5e show cross-plume trace gas concentrations over the center of Nashville at midafternoon (~1540 LT). The peak O<sub>3</sub> concentration in the center of the plume has risen to 130 ppbv from the 70 ppbv maximum observed during late morning. The relatively high NO<sub>x</sub> concentration exhibited in Figure 5e indicates the potential for forming substantial additional O<sub>3</sub>. The slope of the NO<sub>y</sub>/CO regression, Figure 5f,

indicates some losses of NO<sub>x</sub> oxidation products relative to Figure 5c. Figures 5g and 5h show properties of the urban plume about 30 km southwest of Nashville at ~1500 LT. The peak O<sub>3</sub> concentration is similar to the downtown value, but the plume has low potential for forming additional O<sub>3</sub> because of the low NO<sub>x</sub> concentration, Figure 5h. The regression slope of NO<sub>y</sub> versus CO is significantly larger than either of the source region transects consistent with much higher fractional losses of NO<sub>x</sub> oxidation products.

**Figure 6.** Results of box model calculations for conditions in downtown Nashville on July 11, 1995. (a) Instantaneous ozone production rate as a function of the measured hydrocarbon to NO<sub>x</sub>, OH reactivity. Points marked with a diamond were collected mid-to-late morning, solid circles in the midafternoon, and triangles late afternoon. (b) Instantaneous ozone production efficiency as a function of the ratio of the hydrocarbon to NO<sub>x</sub>, OH reactivity. Sample designation as for Figure 8a.

**Figure 7.** Calculated instantaneous O<sub>3</sub> production rate as a function of the product of the NO concentration and the square root of the primary radical production rate. Diamonds are calculated for background conditions; solid circles are calculated for the photochemically mature Nashville urban plume. Calculations are driven by measurements made midafternoon on July 11, 1995, by the G-1. The linear dependency exhibited by the data is characteristic of ozone production under NO<sub>x</sub>-limited conditions.

**Figure 8.** Trace gas concentrations in the Nashville urban plume about 5 km south of the urban center at midafternoon on July 12, 1995. (a) O<sub>3</sub> and CO; (b) NO<sub>y</sub> and NO<sub>x</sub>.

**Figure 9.** Effect of the of zeroing isoprene emissions on the characteristics of O<sub>3</sub> production in the Nashville source region and in a region where isoprene concentrations were very high. In the source region, reducing isoprene emissions decreases P(O<sub>3</sub>) and OPE<sub>x</sub> by about 20%. In the high isoprene region, zeroing the isoprene concentration decreases P(O<sub>3</sub>) and OPE<sub>x</sub> by more than a factor of 2 and shifts the system from nominally NO<sub>x</sub>-limited, to nominally hydrocarbon-limited ozone production.

**Figure 10.** Sensitivity of  $P(\text{O}_3)$  to changes in  $\text{NO}_x$  and hydrocarbon concentrations. All data were collected on July 11, 1995. Solid squares represent measurements made in the Nashville source region and include measurements made midmorning to late afternoon. Solid circles represent measurements made in the background; some of these measurements were made under conditions where local sources of  $\text{NO}_x$  were present. Closed triangles represent measurements made in the photochemically mature Nashville urban plume. All of the measurements in the source region exhibit hydrocarbon-limited  $\text{O}_3$  production.  $P(\text{O}_3)$  in the mature urban plume is  $\text{NO}_x$ -limited as is  $P(\text{O}_3)$  for most of the background measurements.

(a)

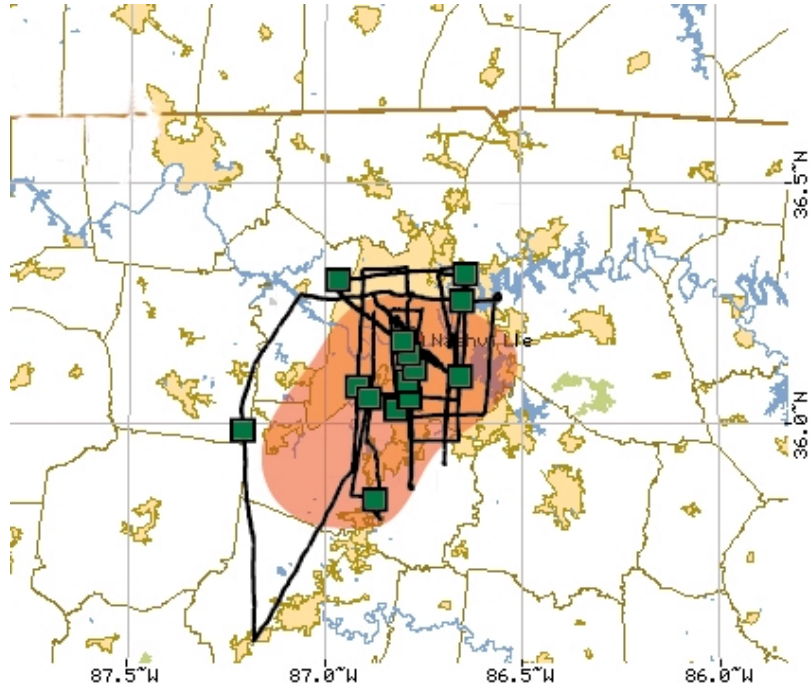
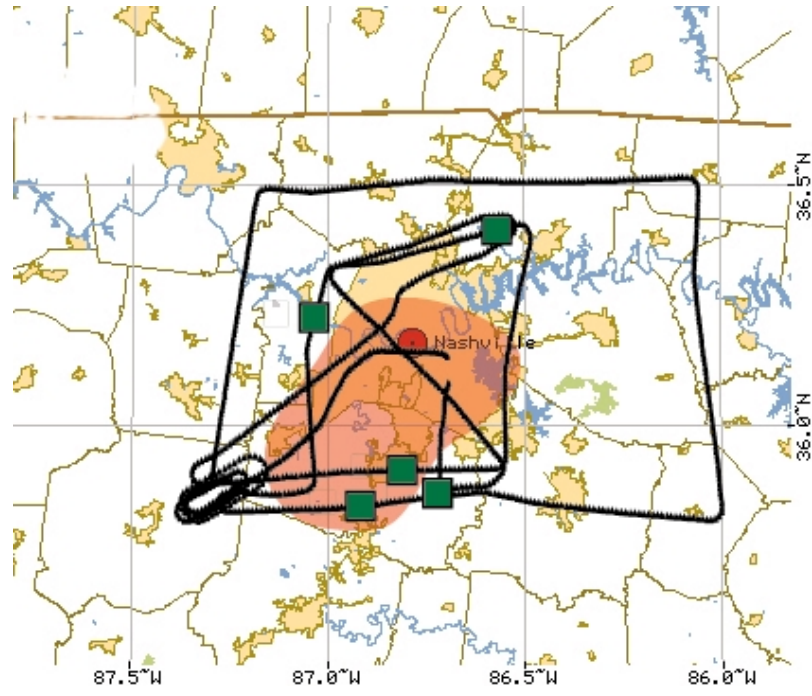


Plate 1a

(b)



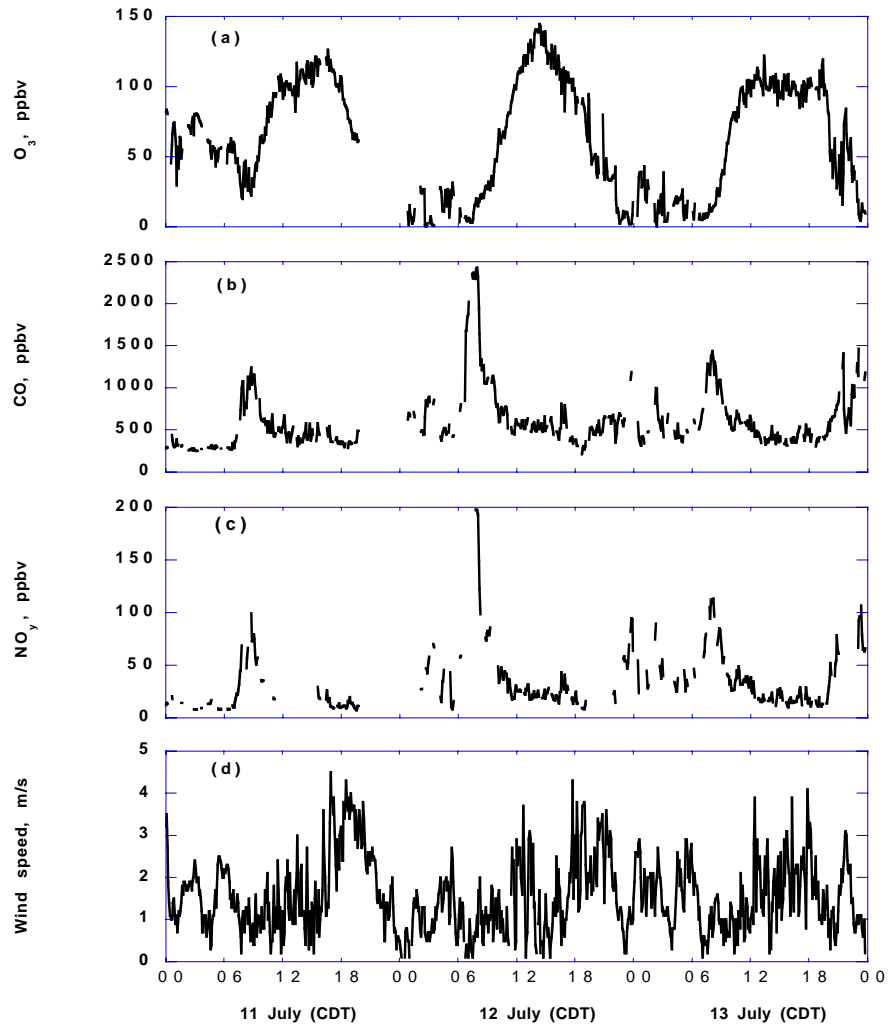


Figure 1

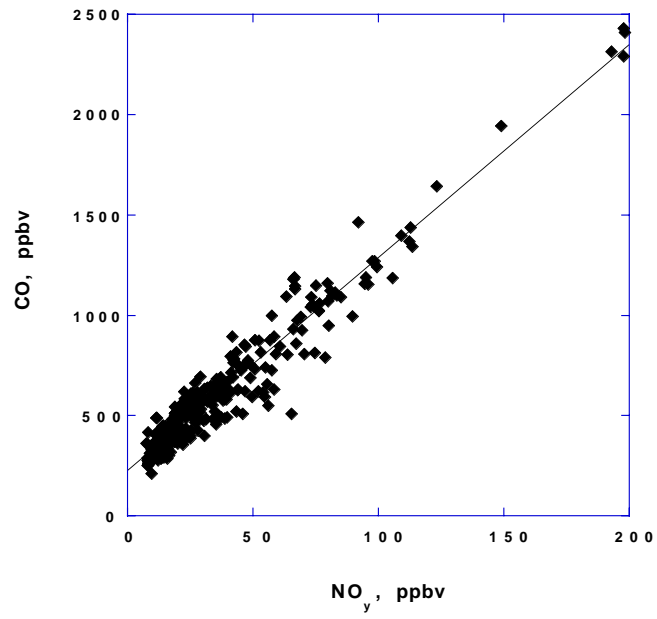


Figure 2

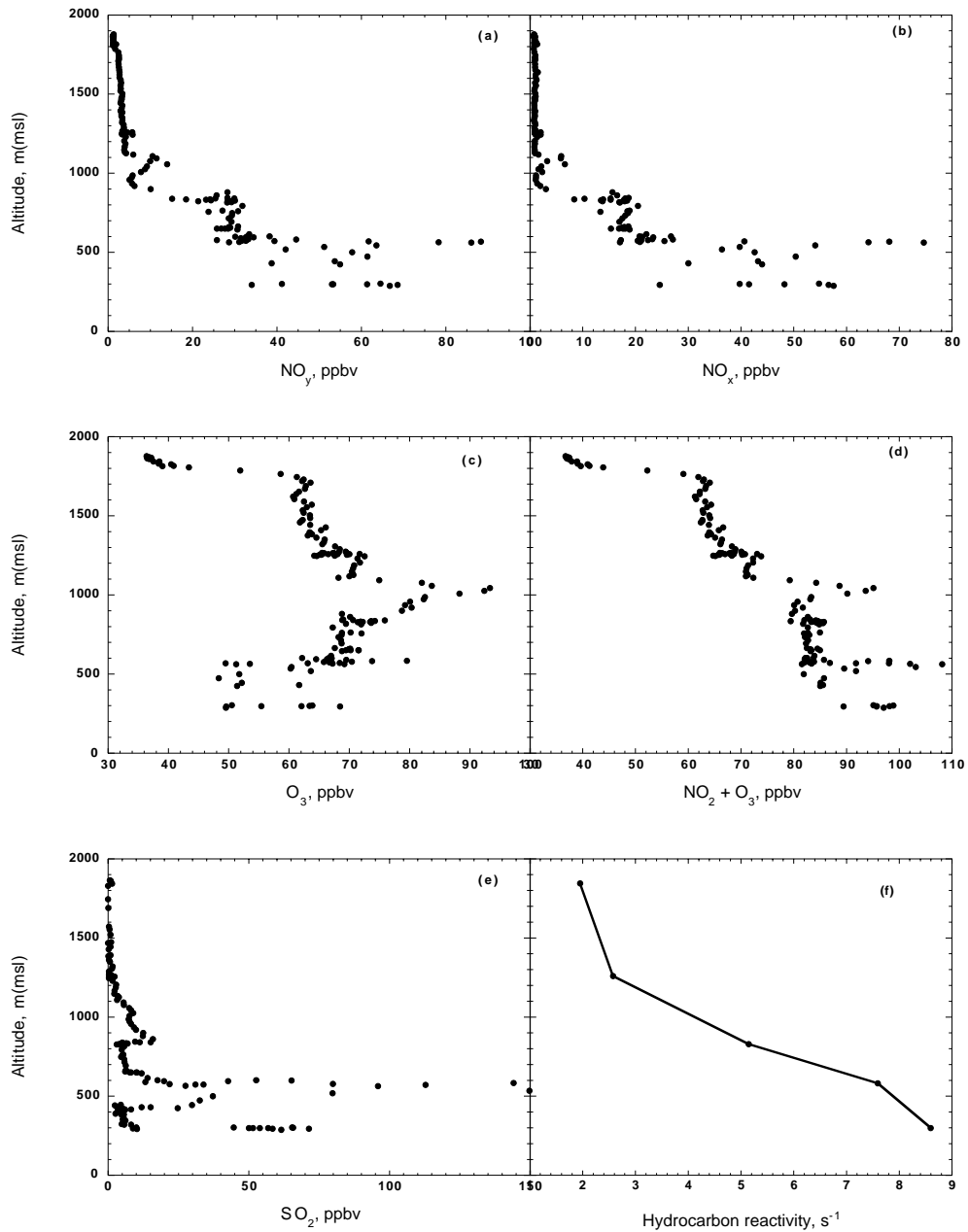


Figure 3

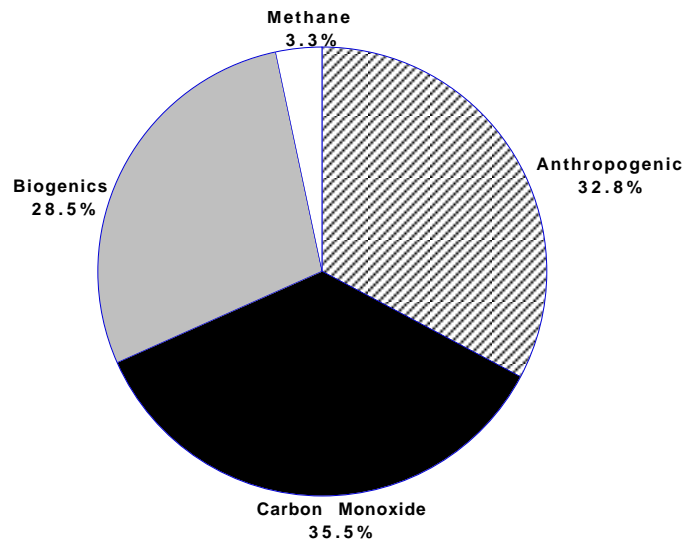


Figure 4

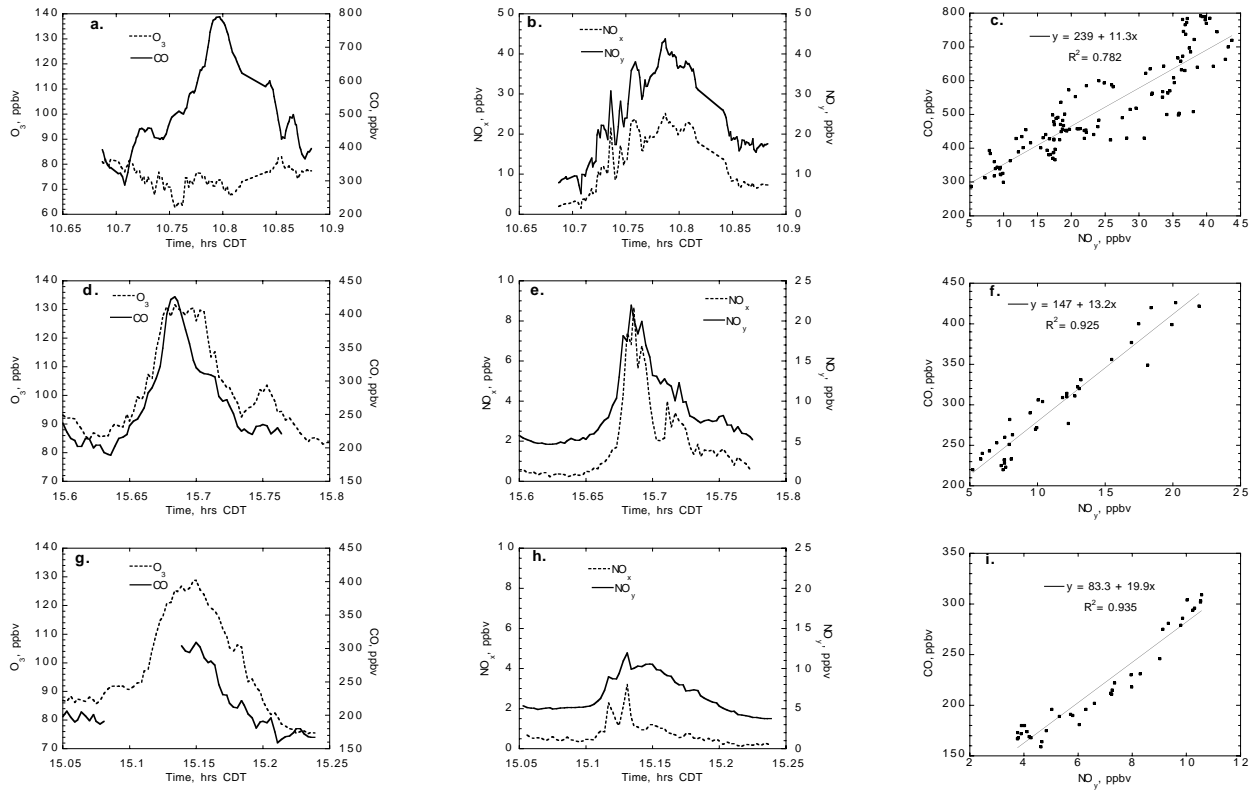


Figure 5

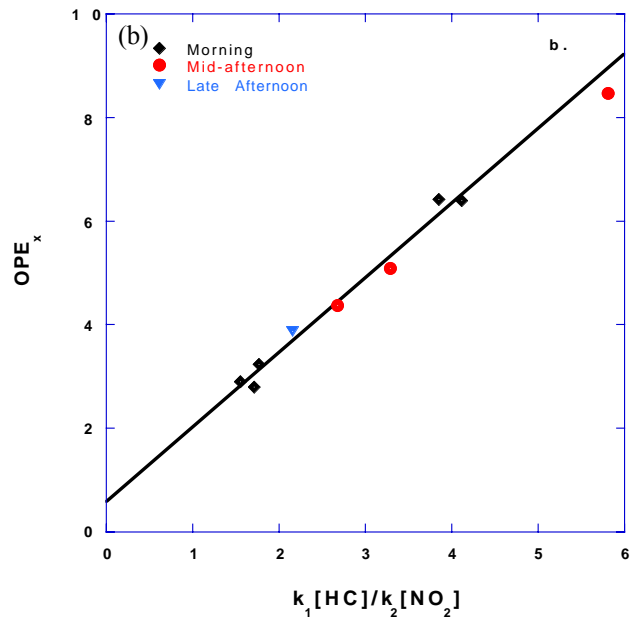
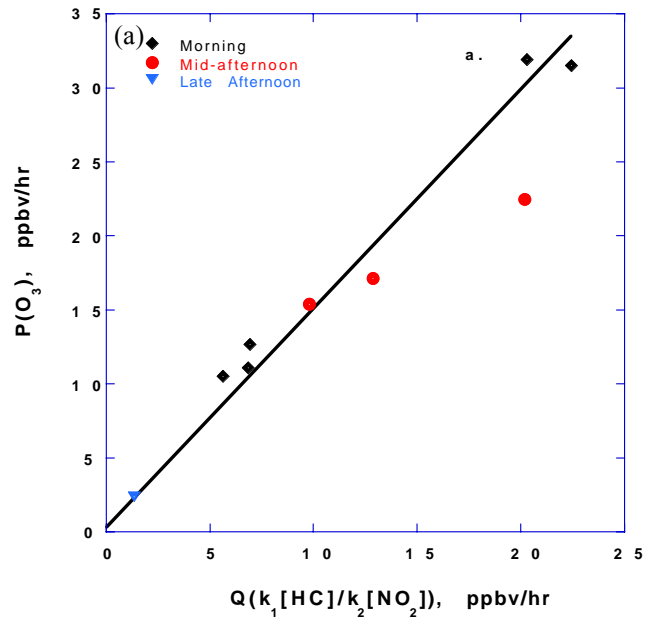


Figure 6

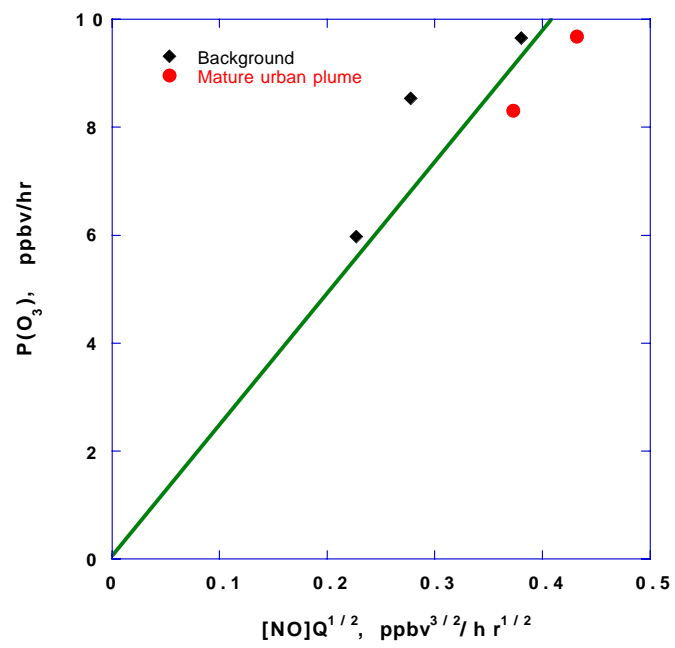


Figure 7

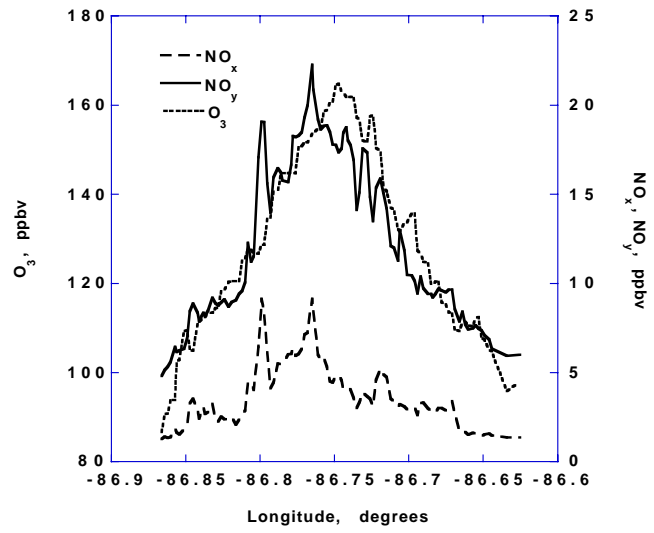


Figure 8

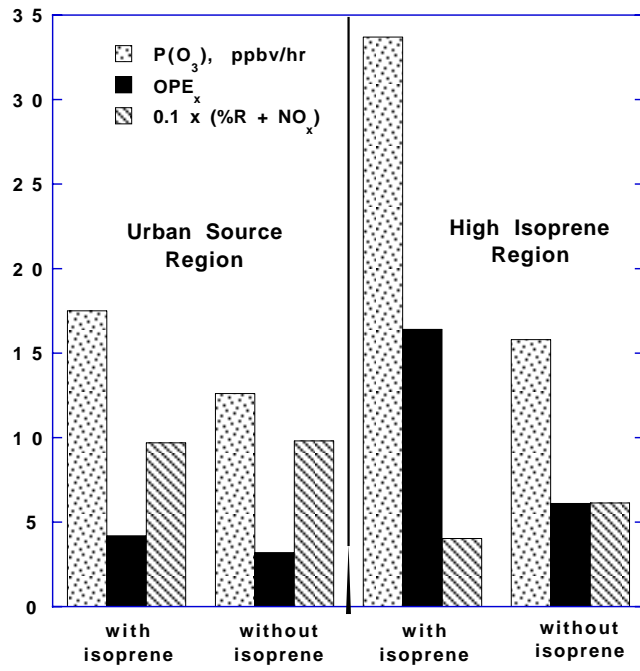


Figure 9

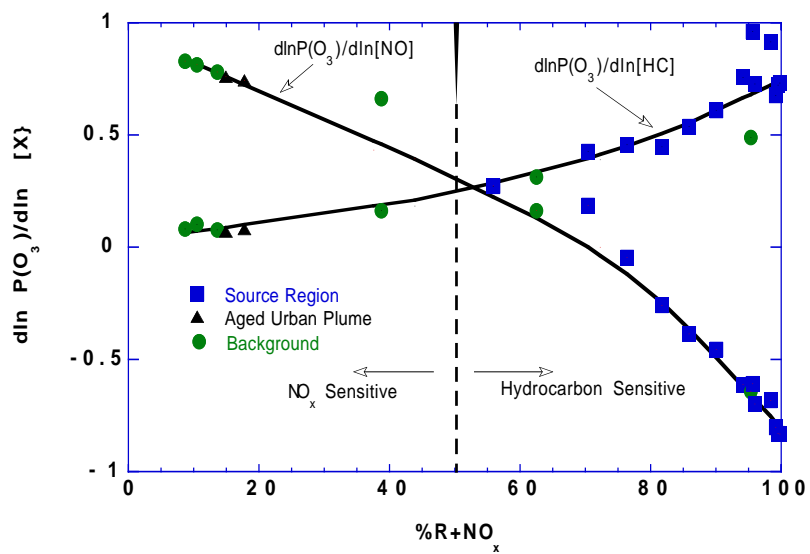


Figure 10